Conventional and Nanometric Nucleating Agents in Poly(ε-caprolactone) Foaming: Crystals vs. Bubbles Nucleation

Carlo Marrazzo,[1] Ernesto Di Maio,[1] Salvatore Iannace[2]
[1] *Department of Materials and Production Engineering, Faculty of Engineering, University of Naples Federico II, P.le Tecchio 80, 80125 Naples, Italy*

[2] *Institute of Composite and Biomedical Materials, National Research Council (IMCB-CNR) P.le E. Fermi 1 Loc. Granatello, 80055 Portici (Na) - Italy*

The aim of this article was to investigate the nucleating ability of different nucleating agents for the foaming of poly(ε-caprolactone), a biodegradable, semicrystalline polymer. In particular, the efficiency of the nucleating agent in inducing the formation of the gaseous phase has been compared to the efficiency in inducing the formation of the crystalline phase. In effect, in foaming of semicrystalline polymers, bubble nucleation and crystal nucleation are concurrent and somehow interacting phenomena. Here, these two aspects have been evidenced and clarified. Foams were prepared by using a batch process with the pressure quench method, with nitrogen and carbon dioxide as the blowing agents. Conventional and novel nucleating agents were used: talc has been compared to several novel nanometric particles of different geometries and dimensions, such as titanium dioxide and alumina powders, exfoliated and intercalated clays, and carbon nanotubes. Foam densities and morphologies, in terms of number of cells per initial unit volume, were measured and found to depend both on crystalline phase nucleation and gaseous phase nucleation. In fact, the different nucleating agents, depending on shape, dimension, and surface functionalization, selectively nucleated the crystallites and/or the bubbles, affecting, respectively, bubble growth (and, hence, final foam density) and bubble nucleation (and, hence, cell number density—morphology). POLYM. ENG. SCI., 48:336–344, 2008. © 2007 Society of Plastics Engineers

INTRODUCTION

In the industrial practice of thermoplastic foaming, it is of vital importance the use of nucleating agents, in order to control the final foam morphology [1, 2]. Traditional nucleating agents are generally made out of talc, which is cheap, efficient, easy to disperse in the polymer, and in large amount to form master batches. Recently, nanometric fillers gained attention, due to the remarkable improvement in some materials properties when compared to the virgin polymer or conventional microcomposites [3, 4]. According to the classical nucleation theory [5], in the foaming process, the heterogeneous nucleation rate is a function of the heterogeneous nucleation sites concentration (defined as the number of particles per cubic centimeter). Therefore, particles concentration is very important because it sets the upper (theoretical) limit for heterogeneous nucleation. With this preface and with the development of nanocomposites, the investigation on possible nanometric nucleating agents for thermoplastic foaming spread in the scientific community. In the scientific literature, however, there is still a certain disagreement on the efficiency of these systems in foaming. For example, Ramesh and Lee expressed these doubts already in the title of their article: "Do nanoparticles really assist in nucleation of fine cells in polyolefin foams?" [6]. They showed that, compared to the more traditional talc filling, organoclay resulted less effective in polypropylene (PP) foaming, despite the higher number of active sites for nucleation. On the contrary, less recent works from the Toyota Technical Institute reported up to two orders of magnitude increase in the cell number densities on a PP/clay system in which foaming was enhanced by the use of a maleic anhydride-functionalized PP [7, 8]. They also reported successful results on a polycarbonate/fluoroectorite system [9] and on two poly(lactic acid)/organoclay systems [10], evidencing the different efficiency of different clay surface modifications to achieve micro to nanocellular foams. In the foaming of polystyrene (PS), Han et al. [11] reported the efficiency of organoclay in comparison with talc, evidencing an improved effect of exfoliated clay with respect to talc and intercalated clay, Tatibouët et al. [12] compared titanium dioxide and talc,

Correspondence to: Ernesto Di Maio; e-mail: edimaio@unina.it
DOI 10.1002/pen.20937
Published online in Wiley InterScience (www.interscience.wiley.com).

TABLE 1. List of the nucleating agents used in this study, from producers' datasheets.

	Trade name	Typology	Shape	Characteristic dimension	Producer
Talc	Fintalc M03	Talc	Cubic	1 μm	Mondo Minerals OY (Helsinki, Finland)
Alumina	Aeroxide AluC	Al_2O_3	Spherical	13 nm	Degussa GmbH (Düsseldorf, Germany)
230L	Hombitec RM230L	TiO_2	Spherical	20 nm	Degussa GmbH (Düsseldorf, Germany)
130F	Hombitec RM130F	TiO_2	Spherical	15 nm	Degussa GmbH (Düsseldorf, Germany)
30B-hs	Cloisite 30B	Modified montmorillonite	Platelet	Exfoliated	Southern Clay Products (Gonzales, TX)
30B-ls	Cloisite 30B	Modified montmorillonite	Platelet	Intercalated	Southern Clay Products (Gonzales, TX)
93A	Cloisite 93A	Modified montmorillonite	Platelet	Intercalated	Southern Clay Products (Gonzales, TX)
cn	Aldrich 636509-2G	Carbon nanotubes	Tube	15 nm	Sigma-Aldrich Co. (St. Luois, MO)

reporting significant higher efficiency of talc, and Shen et al. [13] reported the use of carbon nanofibers. Zeng et al. [14] investigated the foaming of nanocomposites based on PS and poly-(methylmethacrylate), evidencing that cell morphology can be manipulated by adjusting the polymer-clay surface-blowing agent interactions. Other examples include polyamides [15], polyurethanes [16], and high-density polyethylene [17]. In all the above works, however, the effective improvement brought about by the nanometric nucleating agent is sometimes unconvincing. It should be also added that many articles often present comparisons among foams with very different final densities (when reported), for which the claimed increase in the cell number density (reported as number of cell per unit final volume, not per unit initial volume) is more likely to be due to the reduced expansion than to the increase in the bubble number. Furthermore, most of the articles do not compare the novel nucleating agents to the traditional, cheaper ones, which are all over the world utilized in foaming.

In this context, the present article is aimed to clarifying the roles and efficiencies of nanometric nucleating agents in the foaming process, by using poly(ε-caprolactone) (PCL) as the experimental semicrystalline model polymer.

MATERIALS AND METHODS

Materials

PCL (CAPA 6800, Solvay, Warrington, UK), a biodegradable aliphatic polyester, was used as the polymeric matrix. The molecular weight and melt flow index are 70,000 g/mol and 7.29 g/10 min (at temperature of 190°C and pressing mass of 2.16 kg), respectively. Its density at room conditions is equal to 1.14 g/cm^3 and characteristic temperatures are $T_g = -60$°C and $T_m = 60$°C.

Nanoparticles of different compositions, with different shapes and/or characteristic dimensions, were used to produce PCL nanocomposites. In addition, a traditional micrometric nucleating agent (talc) was used. The main characteristics of the nucleating agents are reported in Table 1.

Commercial purity grades N_2 and CO_2 (Sol, Monza, Italy) were used as foaming agents in the foaming experiments.

Composites Preparation

Composites based on PCL were prepared by melt-mixing. A Rheomix 600 (Haake, Karlsruhe, Germany) internal mixer with two counter-rotating roller rotors, controlled by the measuring drive unit Rheocord 9000 (Haake), was used for the preparation. A mixing procedure, consisting of three steps, was used in order to achieve a good dispersion of the nucleating agent in the polymeric matrix [18]. In the first step, the polymer was loaded into the mixing chamber at 70°C and rotor speed of 5 rpm. In the second step, the molten polymer was cooled down to increase the viscosity and, hence, stresses associated with flow. When the viscosity was high enough (as revealed by the torque increase), the nucleating agent was mixed to the molten polymer for 12 min at 100 rpm. The torque and temperature histories of a typical mixing process are reported in Fig. 1.

One system, namely the PCL/30B, was also processed for 3 min at rotor speed of 80 rpm in the third step, to investigate the effect of particles dispersion. This system is indicated as 30B-ls (low shear), while the PCL/30B system mixed as previously illustrated is indicated as 30B-hs (high shear). As evidenced in [18], the procedure for producing the 30B-hs is suitable for achieving an exfoliated structure, while the milder mixing process used for the 30B-ls led to an intercalated structure.

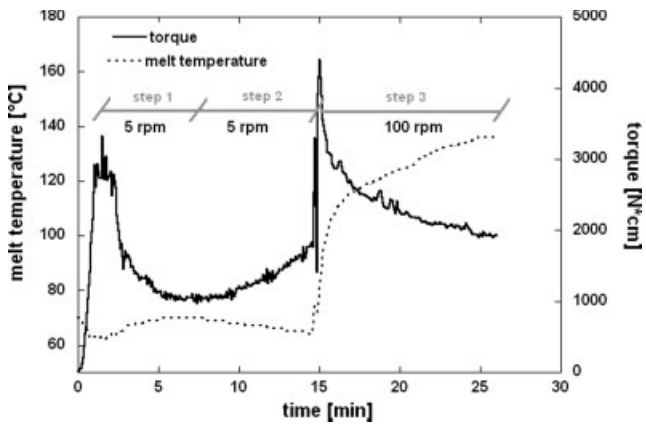

FIG. 1. Melt temperature and torque histories during a typical melt-mixing process.

Composites with 0.1, 0.4, 0.7, and 1 wt% of nucleating agents were prepared. Neat PCL was subjected to the same mixing procedure for proper comparison.

Finally, all the composites were compression molded at 100°C to obtain 3-mm plates for thermal analysis and batch foaming experiments.

Thermal Analysis

Differential scanning calorimetry was performed by using a DSC2920 (TA Instruments, New Castle, DE) to measure the effect of the nucleating agent on the crystallization of PCL. Samples were heated up to 100°C and were kept for 5 min at 100°C to allow complete melting of the polymer. Then, samples were quenched to 45°C, where they were allowed to crystallize isothermally [19].

Foaming Experiments

All the composites were foamed by using a batch foaming apparatus consisting of a thermo regulated and pressurized cylinder having a volume of 0.3 L (model BC-1, HiP, Erie, PA), equipped with different systems for precisely controlling temperatures, pressures and pressure drop rates, which have been thoughtfully described in [20]. Foaming experiments were conducted on cylindrical samples with a diameter of 15 mm, 3 mm in thickness. Samples were saturated with the blowing agent for 6 h, at saturation temperature of 82°C and pressures of 12.5 or 6.0 MPa, depending on the blowing agent (N_2 or CO_2, respectively). After saturation, samples were cooled to the foaming temperature with a controlled, repeatable cooling history, and finally pressure quenched to ambient pressure. The pressure drop rates were 22 MPa/s in the case of N_2 and 17 MPa/s in the case of CO_2. PCL/N_2 systems were foamed in the range 45–52°C, while PCL/CO_2 systems were foamed at 30°C.

Foam Characterization

Densities of foams were measured according to ASTM D-792, by weighting the sample in air and water.

The microstructures were investigated by scanning electron microscopy (SEM S440, Leica Microsystems GmbH, Wetzlar, Germany). Samples were cut in liquid nitrogen and coated with gold using a sputter coater (SC500, Emscope Laboratories, Ashford, UK). SEM images containing at least 100 cells were analyzed to determine the number of cells per cubic centimeter of the unfoamed polymer by using *Eq. 1* [21]:

$$N_0 = \left[\frac{nM^2}{A}\right]^{3/2}\left[\frac{\rho_{neat}}{\rho_{foam}}\right], \quad (1)$$

where n is the number of cells in the micrograph, M and A are respectively the magnification factor of the micrograph and its area, ρ_{neat} and ρ_{foam} are the densities of unfoamed and foamed materials, respectively. Five different zones of the sample under investigation were observed to determine a mean value of the cell number density.

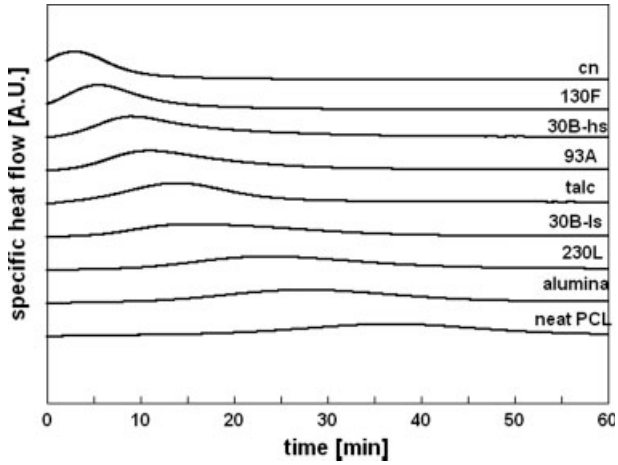

FIG. 2. Isothermal hot-crystallization at 45°C for the 0.4 wt% composites.

RESULTS AND DISCUSSION

Crystals Nucleation—Foam Density

The effect of the nucleating agents on the isothermal crystallization of PCL is reported in Fig. 2 for the 0.4 wt% composites. Curves were shifted vertically for an easier reading of results, ordered by the "nucleating efficiency", described as the ability of the additive (crystalline phase nucleator) to enhance the crystallization kinetics, by reducing the induction time for crystal nucleation (shift of the crystallization peak to the left, in Fig. 2) and by increasing the rate of crystal growth (sharpening of the crystallization peak). Results indicate that the most relevant nucleating efficiency was achieved with the carbon nanotubes, with talc having an intermediate efficiency and clays having, plausibly, a dispersion-related effect. In fact, as observed in an earlier study from our group [18], Cloisite 30B can be successfully exfoliated by melt-mixing with PCL, while 93A can not, and this difference resulted in different crystallization rates. The effect of intercalated Cloisite 30B (30B-ls) was even lower than 93A. As also observed by Zeng et al. [14], polymer/clay interactions have an important effect on the crystalline phase nucleation and, since the Cloisite 30B and 93A have different ionic modification, we do not ascribe the observed differences solely to particles dispersion. Additional analyses could be of help in this case, by giving information on the nature and the intensity of the interactions and on their effect on the crystal nucleation phenomena.

The different crystal nucleating ability of the particles employed in this work is very remarkable, as shown by the isothermal curves in Fig. 2. Based on these results, an

 DOI 10.1002/pen

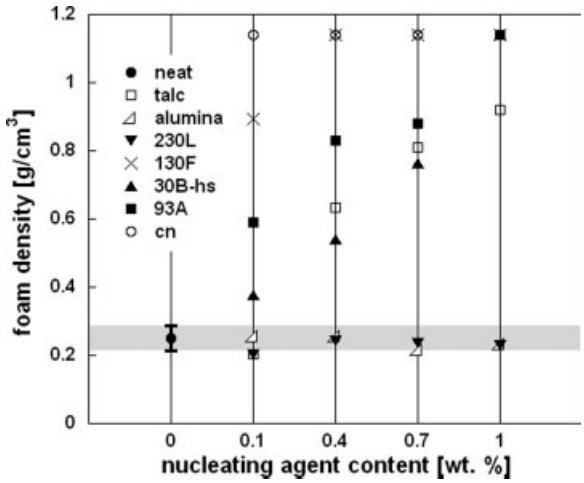

FIG. 3. Effect of concentration of the nucleating agents on the foam densities of PCL-based systems, foamed with N_2 at 46.5°C.

effect on the final foam densities can be expected, since thermal histories of the composites, in foaming and in crystallization, have some similarities. In particular, in batch foaming experiments as well as in isothermal crystallization experiments, cooling from the melt to the foaming temperature (crystallization temperature) is imposed. Therefore, when cooling the polymer-gas solutions to the foaming temperature, if this temperature is low enough to induce the formation of the crystalline phase, subsequent foaming occurs on a partially crystalline structure, whose higher stiffness will hinder expansion, giving foams with a higher density with respect to foams from amorphous material. In situations were the crystallization kinetic is faster than the processing time prior foaming, a complete crystallization of the polymeric matrix can occur and the polymer does not expand at all. Therefore, depending on the degree of crystallization reached by the polymeric matrix before the release of the pressure in the expansion chamber, one can obtain foams with different final densities.

The crystallization kinetic is also affected by the concentration of nucleating agents. By increasing the content of particles from 0.1 to 1%, we observed an increase of the crystallization rates for several types of particles. As a consequence, the degree of crystallinity of the PCL matrix increased with the increase of particle contents and this resulted in foams of higher densities. Figure 3 reports the effect of concentration of the nucleating agents on the final densities of PCL-based foams produced with N_2 at a foaming temperature of 46.5°C. Neat PCL is reported to (at concentration equal to 0) with the error bar obtained by repeating the experiment five times. As it can be observed, at this foaming temperature the effect of the different nucleating agents can be grouped in three sets. First set (I) includes alumina and 230L, whose effect on foam densification was negligible, since values of foam densities obtained with these two nucleating agents fell within the density range of neat PCL (shadowed area in the figure). Second set (II) of nucleating agents includes talc, 30B-hs and 93A, whose effect on foam density depended on the relative amount and increased with concentration, leading almost to the density of unfoamed PCL (1.14 g/cm^3) at 1wt%. Finally, third set (III) includes 130F and carbon nanotubes which inhibited foaming almost at all concentrations, giving densities close to 1.14 g/cm^3.

By comparing these results to those reported in Fig. 2, it can be evidenced that (a) alumina and 230L (I) had the minimum effect on PCL crystallization, (b) 130F and carbon nanotubes (III) led to the fastest crystallization kinetics, and (c) talc, 30B-hs, and 93A (II) had an intermediate behavior. In fact, when cooling the expanding matter to the foaming temperature, the occurrence of crystallization causes a sudden increase of the elasticity of the matrix, reducing its deformability even at very low degree of crystallization [22] and, eventually, inhibiting foaming. At foaming temperature of 46.5°C, the neat polymer starts to crystallize after 30 min ca.; the use of nucleating agents, conversely, by inducing faster crystallization, makes the polymer to partially crystallize just before foaming, restraining deformability and leading to high density systems, to an extent that depends on the nucleating agent type and content. It is important to emphasize that the relative effect of the nucleating agents on the foam density follows the "efficiency order" observed in the isothermal crystallization tests, which proves that the foam densification reported in Fig. 3 is correlated to the polymer crystallization prior foaming.

In effect, for some nanocomposites, the foaming temperature of 46.5°C was too low and extensive crystallization occurred before the available gas could inflate the bubbles to decrease the density. At higher temperatures, crystallization rate could be significantly reduced and/or completely suppressed and relatively lower densities could be achieved. This behavior was observed in foams expanded at 49.5°C. Figure 4 reports density measurement

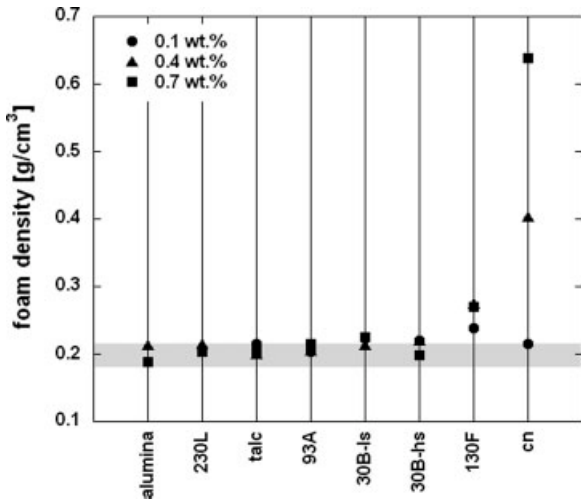

FIG. 4. Effect of typology of the nucleating agent on the foam densities of PCL-based systems, foamed with N_2 at 49.5°C.

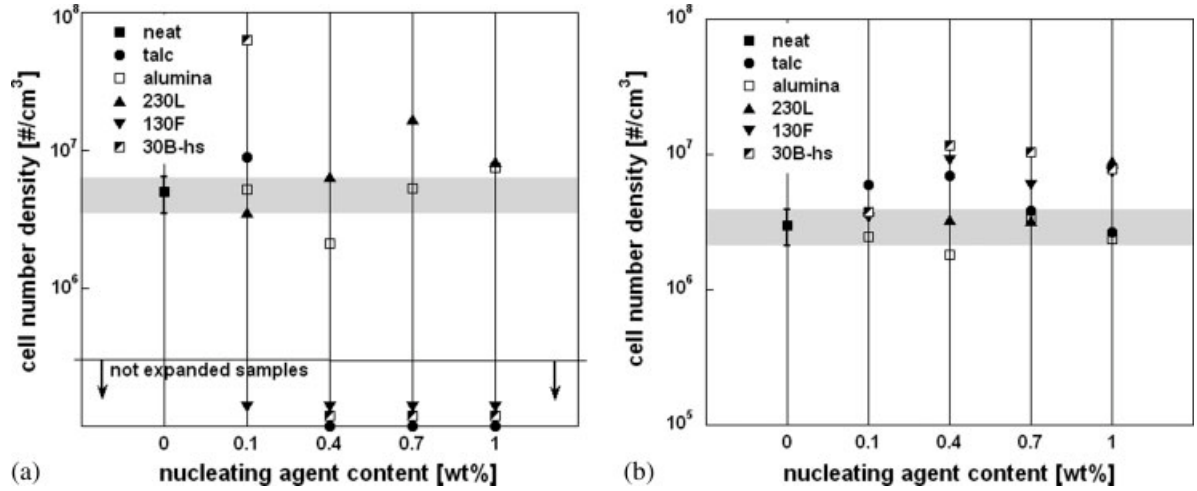

FIG. 5. Cell number densities for selected systems, foamed at 45°C (a) and 47.5°C (b) with N_2.

results obtained on PCL-based composites foamed at foaming temperature just 3°C higher than those reported in Fig. 3. In this case, the foaming conditions allowed foaming for all the investigated systems with foam densities comparable to the density of neat PCL (shadowed area in Fig. 3). Again, the "nucleating efficiency order" is kept and, at higher loading (>0.7 wt%), 130F and nanotubes almost inhibited foaming.

Bubbles Nucleation—Foam Morphology

The effects of the different nucleating agents on the nucleation ability of bubbles can be observed in Fig. 5, where cell number densities per unit initial volume of the composites are reported for selected samples, expanded at 45°C (Fig. 5a) and 47.5°C (Fig. 5b). Again, neat PCL is reported to, for comparison. The first thing to notice is that the "several orders of magnitude increase" in the cell number density, often reported to in the literature [11–17, 23–25], was not observed in our systems. The most relevant bubble nucleation effect was observed for the exfoliated PCL nanocomposites based on clay 30B (sample 30B-hs) containing 0.1% of nanoclay. In this case, the cell density was an order of magnitude higher than neat PCL (shadowed area). It is interesting to observe that, when the concentration of clay increased from 0.1 to 0.4%, the PCL based nanocomposites did not expand at all. These samples are reported to, in the figure, at the bottom, to evidence the effect of concentration (not expanded samples). This was due, as discussed above, to the increased crystallization rate of the polymer that did not allowed the expansion of the polymer. A similar behavior was observed for talc. In this case, samples containing 0.1% of talc showed a cell nucleation density similar to that of the neat PCL while, also in this case, at higher talc loading (0.4%) the increase of crystallization rate led to not expanded materials. Negligible bubble nucleation efficiency was also observed for nanocomposites based on spherical particles of Al_2O_3 and TiO_2 (230L).

With the aim of better clarifying the role of nanoparticles on the heterogeneous bubble nucleation mechanism further investigations were performed at higher foaming temperature, in order to reduce and, eventually, eliminate the occurrence of crystallization prior foaming. As an example, Figure 5b reports the effect of nucleating agent concentration on the cell nucleation density at 47.5°C for the same samples reported in Fig. 5a. In this case, all the samples were foamed and relatively low densities were obtained. Also, in this case we did not observed the increase of several orders of magnitude in the cell nucleation density but only minor effects. This behavior can be explained by considering that the utilized pressure release rate (pressure drop rate) was very high, from 17 to 22 MPa/s. As reported to in the literature [5, 21, 26], the increase of the pressure drop rate reduces the utility of the nucleating agents, by enhancing the homogeneous nucleation rates. Probably, at lower pressure drop rates, the effect of the bubble nucleating agents would have been more relevant, with heterogeneous nucleation rate becoming dominant over the homogeneous nucleation rate but we did not investigated this aspect in this work.

It is however interesting to observe that the highest cell nucleation density was obtained for nanocomposites based on nanoclays. These layered silicates, once exfoliated in the polymeric matrix, can modify the gas solubility and the local diffusivity close to the nanoclay particles. As reported elsewhere [27], the solubility of the gas increases in this nanocomposites, with a possible accumulation of gas molecules in clusters at the interphase between the polymer and the clays. This can be justified by the presence of the organo-modifiers that are usually employed to facilitate the exfoliation of the clay. These small organic salts modify the local thermodynamic around the exfoliated clays resulting in different local gas solubility. Moreover, due to the particular geometry of

 DOI 10.1002/pen

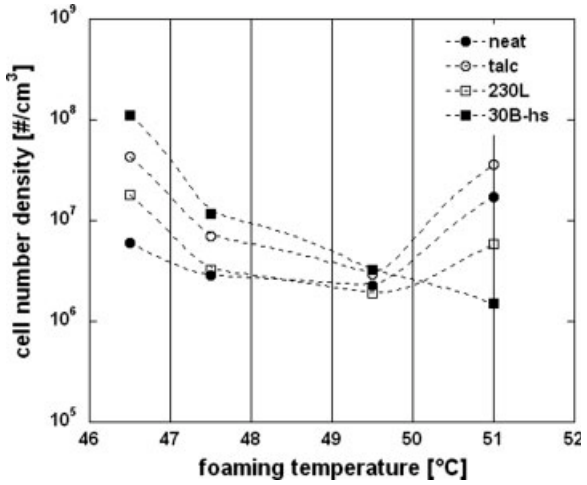

FIG. 6. Effect of foaming temperature on the cell number densities of selected composites containing 0.4 wt% of nucleating agent and expanded with N_2.

the clays, diffusivity of the blowing gas is reduced [27] and therefore homogeneous nucleation can be affected.

Another important point is that the "efficiency order" evidenced for the crystal nucleating effect is, as expected, not retained. In fact, the physical and chemical phenomena beneath nucleation of bubbles are different from ones for the nucleation of crystals. One soon recognizes that here things are more complex, with respect to the induction of crystallinity. To verify this, it is useful to analyze the effect of the temperature on foam morphology, as illustrated in Figures 6 and 7, which report the effect of the foaming temperature on cell number density and on foam density, respectively, for selected PCL/nucleating agent systems. Figure 6 shows that bubbles nucleation strongly depends on the foaming temperature. Most of the samples showed a reduction of the cell density from 46.5 to 49.5°C and, then, an increase at 51°C (except for the nanocomposites based on exfoliated nanoclays). In the same range of temperature, we observed a remarkable reduction of the foam density, which was more evident in samples containing talc and exfoliated clays (Fig. 7). As already reported in Fig. 4, neat PCL and the micro/nanocomposites containing talc, Al_2O_2 (230L) and exfoliated clay (30B-hs) showed approximately the same density at temperatures from 49.5 to 53°C.

By a comparative analysis of these two sets of data (Figs. 6 and 7) we can draw some considerations regarding the role of the micro and nanoparticles for the heterogeneous bubble nucleation in correlation with their role in the nucleation of the PCL crystalline phase. First, at higher temperatures, where densities are all pretty much the same, differences in the cell number densities are solely due to the different bubble nucleating effect of the different nucleating agents while at lower temperatures, there is a strong interplay between the nucleating agents and the newly formed crystals, which behave as bubble nucleating agent themselves [25]. Figure 6, in effect, shows that, at low temperature 30B-hs and talc allowed the nucleation of a greater number of bubbles with respect to the neat PCL and 230L. Figure 7, however, indicates that this increase is mainly due to the presence of crystals, responsible for the densification observed at the same temperature for 30B-hs and talc systems. At higher temperatures, when foam densities are pretty much the same (Fig. 7), the role of the nucleating agents for the bubbles becomes evident and can be univocally ascribed to the nucleating agent (not to crystals, which are not present).

Furthermore, comparison between Figs. 6 and 7 proves that, at sufficiently high temperatures where crystallization does not affect foaming, the effect of cell number density on foam density is negligible. In fact, at 51°C we obtained foams of equal density (Fig. 7) characterized by different number of cells of different size (Fig. 6). Despite the different morphologies achievable with the use of the different nucleating agents, foam densities of PCL systems do not change and these results suggested that foam density depends mostly on the blowing agent availability (solubility) and, to a minor extent, on processing parameters. In effect, as far as the polymer is able to contain the blowing agent (no cells rupture) and as far as the processing parameters (mostly, temperature) allows the deformation of the polymer (expansion), the foam can grow, independently of the number of cells, blown by the gas solubilized in the polymeric phase. Morphology may affect density only, to a limited extent, when it helps the structure to bear its own weight (no cell collapse) or to retain the blowing agent (no external cell wall rupture) [28].

To summarize, the nucleation of bubbles can be induced by both the presence of micro and nanoparticles and by the presence of the polymeric crystals. The relative importance of these two mechanisms depends on: (a) the foaming temperature, (b) the kind of nucleating agent, (c) the number and dispersion of the particles, and (d) by the different surface interactions between the species which can, in turn, eventually be affected by the blowing

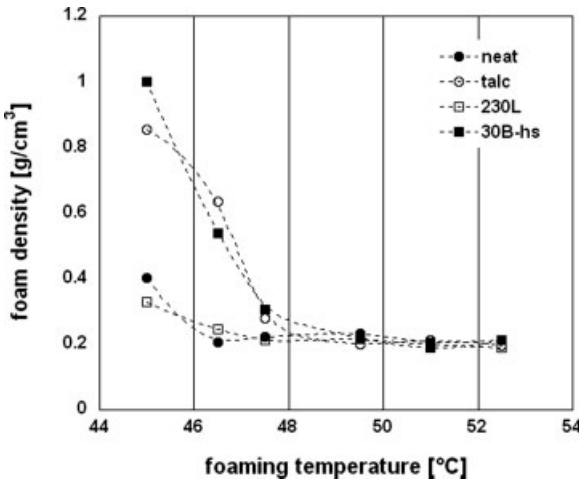

FIG. 7. Effect of foaming temperature on the foam densities of selected composites containing 0.4 wt% of nucleating agent.

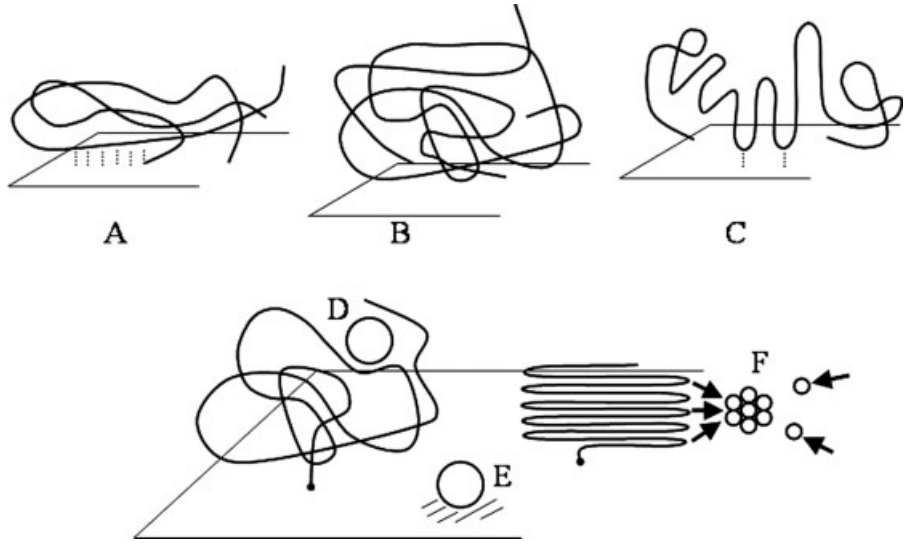

FIG. 8. Schematic of possible interactions among the polymer, the nucleating agents and the gaseous phase taking part in crystallization and foaming.

agent. To describe this complex situation, Fig. 8 illustrates the possible scenarios resulting from the interactions among the molten polymer, the gas, and the nucleating agent. For the sake of simplicity, in this scheme, flat surfaces represent the solid particles surfaces, whether they are spherical, flat or cylindrical.

In crystallization, depending on the number of particles, on their dispersion and on the surface interaction between the particles and the polymer, three situations (A, B, and C) are possible, whether the particle retards, does not influence, or accelerates the crystalline phase nucleation, respectively. Eventually, the gas solubilized in the polymer may affect these interactions and relative effects.

In foaming, depending on the temperature, the surface interactions and the local availability of gaseous molecules, bubbles can preferentially nucleate in the polymeric bulk (homogeneous nucleation, D), on the surface of the particles (heterogeneous nucleation, E) or on the surface of the crystalline phase (heterogeneous nucleation, F).

These schemes/assumptions have been reported in the literature on foaming of nanocomposites and on crystallization of nanocomposites by several authors [25, 29–33] to which we suggest the reader to refer for a further insight into the phenomena. Reported mechanisms include: (i) simply, the heterogeneous bubble nucleation effect by the additional crystal surface (amorphous/crystal interfaces), as classically described in the context of nucleation theories; (ii) the presence of microvoids associated to the formation of crystals, which could be preferred sites for nucleation; and (iii) the expulsion of gas molecules from the newly formed crystalline phase (in the crystals gas solubility is negligible) which form volumes of higher gas concentration in the very vicinity of the crystal surface, inducing a reduction of the thermodynamic barrier to nucleation and a correspondent increase of the nucleation rate. Here, however, we would like to evidence the tight link between crystallization and bubble nucleation and the possible scenarios (when A–C and D–F are combined) in foaming of semi crystalline polymers. In effect, depending on (i) the particle shape, (ii) their size and size distribution, (iii) the surface interaction with the polymer and the blowing agent, (iv) the availability of the blowing agent, and (v) the processing parameters (both temperature and pressure drop rate), different combinations are possible, determining the relative importance of the phenomena and, finally, defining the final foam structure. For the systems reported in this work, mechanism F occurs in most of the foams expanded at temperature lower than 49.5°C. In these conditions, crystallization is favored by the presence of the heterogeneous micro and nanosurfaces. At temperature equal or higher than 49.5°C, mechanisms E and D seem to control the nucleation of the bubbles.

To verify the effect of the type of gas, foaming attempts were performed by using CO_2 as blowing agent. CO_2, as known, is rather different from N_2 for the polarity, the higher compressibility and the resulting different plasticizing effect on the polymers [34, 35]. It should, from one hand, modify the surface interaction among the different species and, from the other hand, shift somehow the relative importance of the two nucleation phenomena. In fact, Fig. 9 reports the comparison between CO_2 and N_2 in foaming the different composites, evidencing relevant differences. In particular, in CO_2-PCL foaming, the effect of the nucleating agents on the nucleation of bubbles resulted relatively more important than in the case of N_2 and allowed the achievement of cell number densities (when using 130F and 230L) comparable with N_2-PCL foams, with a relative increase of 1.5 orders of magnitude with respect to the neat polymer. In this case, the mechanism E illustrated in Fig. 8 is most plausible mechanism.

 DOI 10.1002/pen

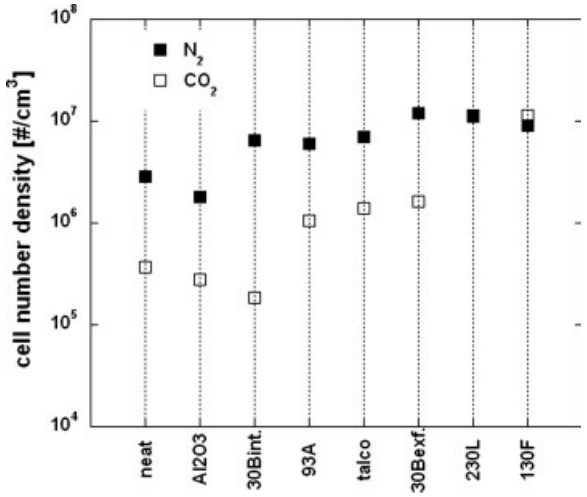

FIG. 9. Effect of the nucleating agent (at 0.4 wt%) on the cell number densities; comparison between N_2 and CO_2 as the blowing agent, foamed at 47.5°C and 30°C, respectively.

To complete the above discussion and to answer to the question posed in the introduction, selected SEM micrographs are reported in Fig. 10. In particular, the cellular morphology of PCL and PCL nanocomposite containing 0.4% of spherical TiO_2 (130F) were chosen as examples of the different mechanisms discussed above.

Figure 10a and c, report the SEM micrographs of PCL and PCL with 0.4% 130F, respectively, both foamed with CO_2 at 30°C. The final densities of these two foams were almost the same and equal to 0.12 and 0.16 g/cm^3 for the neat PCL and the nanocomposite, respectively. These results suggested that, in these processing conditions, the neat PCL and the nanocomposite did not crystallize prior foaming, and that the nanoparticles did not promote any nucleation of crystals. However, the foam from the nanocomposite showed a cellular morphology characterized by a higher number of smaller cells, suggesting the presence of a heterogeneous nucleation mechanism and, therefore, the efficiency of 130F as bubble nucleating agent (mechanism E in Fig. 8). Figure 10b and d compare the cellular morphologies of the same materials (neat PCL and the 0.4% 130F based nanocomposite) but foamed with N_2 at 47.5°C. In this case, even though the foaming temperature is much higher than in the CO_2 case, the 130F nanoparticles promoted premature crystallization before foaming leading to foams of higher density (0.62 g/cm^3) compared to neat PCL (0.23 g/cm^3). In this case, the higher number of

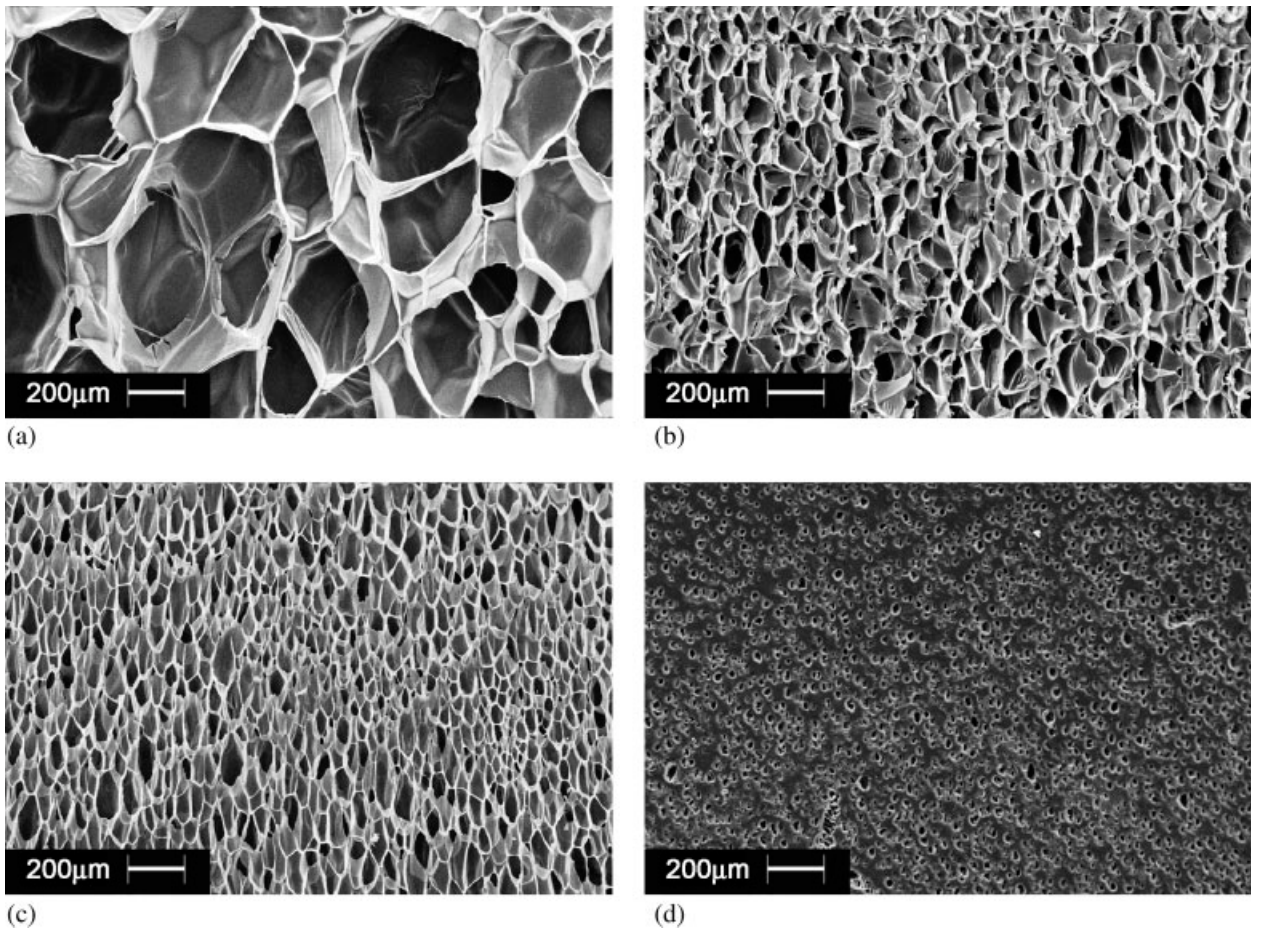

FIG. 10. SEM micrographs of foams from neat PCL and PCL with 130F (0.4 wt%) expanded with CO_2, foaming temperature 30°C (a and c, respectively) and N_2, foaming temperature 47.5°C (b and d, respectively).

cells can be therefore related to a combination of mechanisms F and E (Fig. 8).

In conclusion, the analysis of the cellular morphologies of these selected systems indicate that the improvement brought about by the use of nanometric nucleating agents is effectively an improvement of the foamed structures only when bubbles nucleating efficiency is proved (compare Fig. 10a and c) in contrast to other side effects (e.g.: densification observed in Fig. 10d as compared to Fig. 10b).

This topic is, anyway, still wide-open, and theoretical and experimental studies should be done in order to deeply understand the role of nanometric particles, and, more generally, of the nucleating agents (and of their size, geometry and surface properties) in the nucleation of bubbles in polymeric foaming, and, eventually, in the presence of crystal embryos.

CONCLUSIONS

The effects of conventional and nanometric particles as nucleating agents for PCL foaming were investigated. Both crystalline phase nucleation and bubble nucleation, induced by the presence of the nucleating agents, strongly affected foaming and are intimately correlated. These effects were found to depend on the type, dimension, shape, and surface functionality of the nucleating agent and on the blowing agent and temperatures used for foaming. In particular, the different PCL-nucleating agent systems showed selective nucleation efficiencies, depending strongly on the blowing agent (which has effect on the surface interaction between the polymer and the particle) and on the temperature (which can modify the relative importance of the two nucleation phenomena). By fine-tuning the processing parameters and the nucleating agent, the final foam performances, in terms of foam density and morphology, can be optimized. Among the nanoparticles employed in this work, the most efficient bubble nucleation was achieved by using 0.4 wt% nanometric titanium dioxide with CO_2, with an increase of almost two orders of magnitudes in the cell number density with respect to the neat polymer.

REFERENCES

1. Y. Fujimoto, S.R. Simha, M. Okamoto, and A. Ogami, *Macromol. Rapid Commun.*, **24**, 457 (2003).
2. M. Mitsunaga, Y. Ito, S.S. Ray, M. Okamoto, and K. Hironaka, *Macromol. Mater. Eng.*, **288**, 543 (2003).
3. M. Alexandre and P. Dubois, *Mater. Sci. Eng.*, **28**, 1 (2000).
4. E.P. Giannelis, R. Krishnamoorti, and E. Manias, *Adv. Polym. Sci.*, **138**, 108 (1999).
5. J.S. Colton and N.P. Suh, *Polym. Eng. Sci.*, **27**, 485 (1987).
6. N.S. Ramesh and S.T. Lee, *Cell. Polym.*, **24**, 269 (2005).
7. M. Okamoto, P.H. Nam, P. Maiti, T. Kotaka, T. Nakayama, M. Takada, M. Ohshima, A. Usuki, N. Hasegawa, and H. Okamoto, *Nano Lett.*, **1**, 503 (2001).
8. P.H. Nam, P. Maiti, M. Okamoto, T. Kotaka, T. Nakayama, M. Takada, M. Ohshima, A. Usuki, N. Hasegawa, and H. Okamoto, *Polym. Eng. Sci.*, **42**, 1907 (2002).
9. M. Mitsunaga, Y. Ito, S.S. Ray, M. Okamoto, and K. Hironaka, *Macromol. Mater. Eng.*, **288**, 543 (2003).
10. Y. Fujimoto, S.S. Ray, M. Okamoto, A. Ogami, K. Yamada, and K. Ueda, *Macromol. Rapid Commun.*, **24**, 457 (2003).
11. X. Han, C. Zeng, L.J. Lee, K.W. Koelling, and D.L. Tomasko, *Polym. Eng. Sci.*, **43**, 1261 (2003).
12. J. Tatibouët, R. Gendron, A. Hamel, and A. Sahnoune, *J. Cell. Plast.*, **38**, 203 (2002).
13. J. Shen, C. Zeng, and L.J. Lee, *Polymer*, **46**, 5218 (2005).
14. C. Zeng, X. Han, L.J. Lee, K.W. Koelling, and D.L. Tomasko, *Adv. Mater.*, **15**, 1743 (2003).
15. H. Karbas, P. Nelson, M. Yuan, S. Gong, and L.-S. Turng, *Polym. Compos.*, **24**, 655 (2003).
16. X. Cao, L.J. Lee, T. Widya, and C. Macosko, *Polymer*, **46**, 775 (2005).
17. Y.H. Lee, C.B. Park, K.H. Wang, and M.H. Lee, *J. Cell. Plastics*, **41**, 487 (2005).
18. Y. Di, S. Iannace, E. Di Maio, and L. Nicolais, *J. Polym. Sci. Part B: Polym. Phys.*, **41**, 670 (2003).
19. E. Di Maio, S. Iannace, L. Sorrentino, and L. Nicolais, *Polymer*, **45**, 8893 (2004).
20. C. Marrazzo, E. Di Maio, and S. Iannace, *J. Cell. Plastics*, in press.
21. X. Xu, C.B. Park, D. Xu, and R. Pop-Iliev, *Polym. Eng. Sci.*, **43**, 1378 (2003).
22. H.H. Winter and M. Mours, *Adv. Polym. Sci.*, **134**, 165 (1997).
23. C.B. Park, L.K. Cheung, and S.W. Song, *Cell. Polym.*, **17**, 221 (1998).
24. N.S. Ramesh, D.H. Rasmussen, and G.A. Campbell, *Polym. Eng. Sci.*, **34**, 1698 (1994).
25. J. Reignier, J. Tatibouët, and R. Gendron, *Polymer*, **47**, 5012 (2006).
26. J.S. Colton and N.P. Suh, *Polym. Eng. Sci.*, **27**, 493 (1987).
27. S. Cotugno, *Modellazione termodinamica dei processi di schiumatura di polimeri biodegradabili e fluidi supercritici*, PhD Thesis, University of Naples Federico II, Naples, Italy (2003).
28. J.W.S. Lee, K. Wang, and C.B. Park, *Ind. Eng. Chem. Res.*, **44**, 92 (2005).
29. D.F. Baldwin, M. Shimbo, and N.P. Suh, *J. Eng. Mater. Technol.*, **117**, 65 (1995).
30. S. Doroudiani, C.B. Park, and M.T. Kortschot, *Polym. Eng. Sci.*, **36**, 2645 (1996).
31. Y.P. Handa, Z. Zhang, V. Nawaby, and J. Tan, *Cell. Polym.*, **20**, 241 (2001).
32. J. Lin, S. Shenogin, and S. Nazarenko, *Polymer*, **43**, 4733 (2002).
33. K. Mizoguchi, T. Hirose, Y. Naito, and Y. Kamiya, *Polymer*, **28**, 1298 (1987).
34. E. Di Maio, S. Iannace, G. Mensitieri, and L. Nicolais, *J. Polym. Sci. Part B: Polym. Phys*, **44**, 1863 (2006).
35. E. Di Maio, G. Mensitieri, S. Iannace, L. Nicolais, W. Li, and R.W. Flumerfelt, *Polym. Eng. Sci.*, **45**, 432 (2005).